

PDF hosted at the Radboud Repository of the Radboud University Nijmegen

The following full text is a preprint version which may differ from the publisher's version.

For additional information about this publication click this link.

<http://hdl.handle.net/2066/72497>

Please be advised that this information was generated on 2019-04-25 and may be subject to change.

Search for flavor-changing-neutral-current D meson decays

V.M. Abazov³⁵, B. Abbott⁷⁵, M. Abolins⁶⁵, B.S. Acharya²⁸, M. Adams⁵¹, T. Adams⁴⁹, E. Aguilo⁵, S.H. Ahn³⁰, M. Ahsan⁵⁹, G.D. Alexeev³⁵, G. Alkhazov³⁹, A. Alton^{64,a}, G. Alverson⁶³, G.A. Alves², M. Anastasoie³⁴, L.S. Ancu³⁴, T. Andeen⁵³, S. Anderson⁴⁵, B. Andrieu¹⁶, M.S. Anzelc⁵³, Y. Arnoud¹³, M. Arov⁶⁰, M. Arthaud¹⁷, A. Askew⁴⁹, B. Åsman⁴⁰, A.C.S. Assis Jesus³, O. Atramentov⁴⁹, C. Autermann²⁰, C. Avila⁷, C. Ay²³, F. Badaud¹², A. Baden⁶¹, L. Bagby⁵², B. Baldin⁵⁰, D.V. Bandurin⁵⁹, S. Banerjee²⁸, P. Banerjee²⁸, E. Barberis⁶³, A.-F. Barfuss¹⁴, P. Bargassa⁸⁰, P. Baringer⁵⁸, J. Barreto², J.F. Bartlett⁵⁰, U. Bassler¹⁶, D. Bauer⁴³, S. Beale⁵, A. Bean⁵⁸, M. Begalli³, M. Begel⁷¹, C. Belanger-Champagne⁴⁰, L. Bellantoni⁵⁰, A. Bellavance⁵⁰, J.A. Benitez⁶⁵, S.B. Beri²⁶, G. Bernardi¹⁶, R. Bernhard²², L. Berntzon¹⁴, I. Bertram⁴², M. Besançon¹⁷, R. Beuselinck⁴³, V.A. Bezzubov³⁸, P.C. Bhat⁵⁰, V. Bhatnagar²⁶, C. Biscarat¹⁹, G. Blazey⁵², F. Blekman⁴³, S. Blessing⁴⁹, D. Bloch¹⁸, K. Bloom⁶⁷, A. Boehnlein⁵⁰, D. Boline⁶², T.A. Bolton⁵⁹, G. Borisso⁴², K. Bos³³, T. Bose⁷⁷, A. Brandt⁷⁸, R. Brock⁶⁵, G. Brooijmans⁷⁰, A. Bross⁵⁰, D. Brown⁷⁸, N.J. Buchanan⁴⁹, D. Buchholz⁵³, M. Buehler⁸¹, V. Buescher²¹, S. Burdin^{42,b}, S. Burke⁴⁵, T.H. Burnett⁸², C.P. Buszello⁴³, J.M. Butler⁶², P. Calfayan²⁴, S. Calvet¹⁴, J. Cammin⁷¹, S. Caron³³, W. Carvalho³, B.C.K. Casey⁷⁷, N.M. Cason⁵⁵, H. Castilla-Valdez³², S. Chakrabarti¹⁷, D. Chakraborty⁵², K.M. Chan⁵⁵, K. Chan⁵, A. Chandra⁴⁸, F. Charles^{18,†}, E. Cheu⁴⁵, F. Chevallier¹³, D.K. Cho⁶², S. Choi³¹, B. Choudhary²⁷, L. Christofek⁷⁷, T. Christoudias^{43,†}, S. Cihangir⁵⁰, D. Claes⁶⁷, B. Clément¹⁸, Y. Coadou⁵, M. Cooke⁸⁰, W.E. Cooper⁵⁰, M. Corcoran⁸⁰, F. Couderc¹⁷, M.-C. Cousinou¹⁴, S. Crépe-Renaudin¹³, D. Cutts⁷⁷, M. Ćwiok²⁹, H. da Motta², A. Das⁶², G. Davies⁴³, K. De⁷⁸, S.J. de Jong³⁴, P. de Jong³³, E. De La Cruz-Burelo⁶⁴, C. De Oliveira Martins³, J.D. Degenhardt⁶⁴, F. Déliot¹⁷, M. Demarteau⁵⁰, R. Demina⁷¹, D. Denisov⁵⁰, S.P. Denisov³⁸, S. Desai⁵⁰, H.T. Diehl⁵⁰, M. Diesburg⁵⁰, A. Dominguez⁶⁷, H. Dong⁷², L.V. Dudko³⁷, L. Duflot¹⁵, S.R. Dugad²⁸, D. Duggan⁴⁹, A. Duperrin¹⁴, J. Dyer⁶⁵, A. Dyshkant⁵², M. Eads⁶⁷, D. Edmunds⁶⁵, J. Ellison⁴⁸, V.D. Elvira⁵⁰, Y. Enari⁷⁷, S. Eno⁶¹, P. Ermolov³⁷, H. Evans⁵⁴, A. Evdokimov⁷³, V.N. Evdokimov³⁸, A.V. Ferapontov⁵⁹, T. Ferbel⁷¹, F. Fiedler²⁴, F. Filthaut³⁴, W. Fisher⁵⁰, H.E. Fisk⁵⁰, M. Ford⁴⁴, M. Fortner⁵², H. Fox²², S. Fu⁵⁰, S. Fuess⁵⁰, T. Gadfort⁸², C.F. Galea³⁴, E. Gallas⁵⁰, E. Galyaev⁵⁵, C. Garcia⁷¹, A. Garcia-Bellido⁸², V. Gavrilo³⁶, P. Gay¹², W. Geist¹⁸, D. Gelé¹⁸, C.E. Gerber⁵¹, Y. Gershtein⁴⁹, D. Gillberg⁵, G. Gintler⁷¹, N. Gollub⁴⁰, B. Gómez⁷, A. Goussiou⁵⁵, P.D. Grannis⁷², H. Greenlee⁵⁰, Z.D. Greenwood⁶⁰, E.M. Gregores⁴, G. Grenier¹⁹, Ph. Gris¹², J.-F. Grivaz¹⁵, A. Grohsjean²⁴, S. Grünendahl⁵⁰, M.W. Grünewald²⁹, J. Guo⁷², F. Guo⁷², P. Gutierrez⁷⁵, G. Gutierrez⁵⁰, A. Haas⁷⁰, N.J. Hadley⁶¹, P. Haefner²⁴, S. Hagopian⁴⁹, J. Haley⁶⁸, I. Hall⁶⁵, R.E. Hall⁴⁷, L. Han⁶, K. Hanagaki⁵⁰, P. Hansson⁴⁰, K. Harder⁴⁴, A. Harel⁷¹, R. Harrington⁶³, J.M. Hauptman⁵⁷, R. Hauser⁶⁵, J. Hays⁴³, T. Hebbeker²⁰, D. Hedin⁵², J.G. Hegeman³³, J.M. Heinmiller⁵¹, A.P. Heinson⁴⁸, U. Heintz⁶², C. Hensel⁵⁸, K. Herner⁷², G. Hesketh⁶³, M.D. Hildreth⁵⁵, R. Hirosky⁸¹, J.D. Hobbs⁷², B. Hoeneisen¹¹, H. Hoeth²⁵, M. Hohlfeld²¹, S.J. Hong³⁰, R. Hooper⁷⁷, S. Hossain⁷⁵, P. Houben³³, Y. Hu⁷², Z. Hubacek⁹, V. Hynek⁸, I. Iashvili⁶⁹, R. Illingworth⁵⁰, A.S. Ito⁵⁰, S. Jabeen⁶², M. Jaffré¹⁵, S. Jain⁷⁵, K. Jakobs²², C. Jarvis⁶¹, R. Jesik⁴³, K. Johns⁴⁵, C. Johnson⁷⁰, M. Johnson⁵⁰, A. Jonckheere⁵⁰, P. Jonsson⁴³, A. Juste⁵⁰, D. Käfer²⁰, S. Kahn⁷³, E. Kajfasz¹⁴, A.M. Kalinin³⁵, J.R. Kalk⁶⁵, J.M. Kalk⁶⁰, S. Kappler²⁰, D. Karmanov³⁷, J. Kasper⁶², P. Kasper⁵⁰, I. Katsanos⁷⁰, D. Kau⁴⁹, R. Kaur²⁶, V. Kaushik⁷⁸, R. Kehoe⁷⁹, S. Kermiche¹⁴, N. Khalatyan³⁸, A. Khanov⁷⁶, A. Kharchilava⁶⁹, Y.M. Khazdheev³⁵, D. Khatidze⁷⁰, H. Kim³¹, T.J. Kim³⁰, M.H. Kirby³⁴, M. Kirsch²⁰, B. Klima⁵⁰, J.M. Kohli²⁶, J.-P. Konrath²², M. Kopal⁷⁵, V.M. Korablev³⁸, A.V. Kozelov³⁸, D. Krop⁵⁴, A. Kryemadhi⁸¹, T. Kuhl²³, A. Kumar⁶⁹, S. Kunori⁶¹, A. Kupco¹⁰, T. Kurča¹⁹, J. Kvita⁸, F. Lacroix¹², D. Lam⁵⁵, S. Lammers⁷⁰, G. Landsberg⁷⁷, J. Lazoflores⁴⁹, P. Lebrun¹⁹, W.M. Lee⁵⁰, A. Leflat³⁷, F. Lehner⁴¹, J. Lellouch¹⁶, J. Leveque⁴⁵, P. Lewis⁴³, J. Li⁷⁸, Q.Z. Li⁵⁰, L. Li⁴⁸, S.M. Lietti⁴, J.G.R. Lima⁵², D. Lincoln⁵⁰, J. Linnemann⁶⁵, V.V. Lipaev³⁸, R. Lipton⁵⁰, Y. Liu^{6,†}, Z. Liu⁵, L. Lobo⁴³, A. Lobodenko³⁹, M. Lokajicek¹⁰, A. Lounis¹⁸, P. Love⁴², H.J. Lubatti⁸², A.L. Lyon⁵⁰, A.K.A. Maciel², D. Mackin⁸⁰, R.J. Madaras⁴⁶, P. Mättig²⁵, C. Magass²⁰, A. Magerkurth⁶⁴, N. Makovec¹⁵, P.K. Mal⁵⁵, H.B. Malbouisson³, S. Malik⁶⁷, V.L. Malyshev³⁵, H.S. Mao⁵⁰, Y. Maravin⁵⁹, B. Martin¹³, R. McCarthy⁷², A. Melnitchouk⁶⁶, A. Mendes¹⁴, L. Mendoza⁷, P.G. Mercadante⁴, M. Merkin³⁷, K.W. Merritt⁵⁰, J. Meyer²¹, A. Meyer²⁰, M. Michaut¹⁷, T. Millet¹⁹, J. Mitrevski⁷⁰, J. Molina³, R.K. Mommsen⁴⁴, N.K. Mondal²⁸, R.W. Moore⁵, T. Moulik⁵⁸, G.S. Muanza¹⁹, M. Mulders⁵⁰, M. Mulhearn⁷⁰, O. Mundal²¹, L. Mundim³, E. Nagy¹⁴, M. Naimuddin⁵⁰, M. Narain⁷⁷, N.A. Naumann³⁴, H.A. Neal⁶⁴, J.P. Negret⁷, P. Neustroev³⁹, H. Nilsen²², A. Nomerotski⁵⁰,

S.F. Novaes⁴, T. Nunnemann²⁴, V. O'Dell⁵⁰, D.C. O'Neil⁵, G. Obrant³⁹, C. Ochando¹⁵, D. Onoprienko⁵⁹, N. Oshima⁵⁰, J. Osta⁵⁵, R. Otec⁹, G.J. Otero y Garzón⁵¹, M. Owen⁴⁴, P. Padley⁸⁰, M. Pangilinan⁷⁷, N. Parashar⁵⁶, S.-J. Park⁷¹, S.K. Park³⁰, J. Parsons⁷⁰, R. Partridge⁷⁷, N. Parua⁵⁴, A. Patwa⁷³, G. Pawloski⁸⁰, B. Penning²², K. Peters⁴⁴, Y. Peters²⁵, P. Pétrouff¹⁵, M. Petteni⁴³, R. Piegaia¹, J. Piper⁶⁵, M.-A. Pleier²¹, P.L.M. Podesta-Lerma^{32,d}, V.M. Podstavkov⁵⁰, Y. Pogorelov⁵⁵, M.-E. Pol², P. Polozov³⁶, A. Pompo[~], B.G. Pope⁶⁵, A.V. Popov³⁸, C. Potter⁵, W.L. Prado da Silva³, H.B. Prosper⁴⁹, S. Protopopescu⁷³, J. Qian⁶⁴, A. Quadt^{21,e}, B. Quinn⁶⁶, A. Rakitine⁴², M.S. Rangel², K. Ranjan²⁷, P.N. Ratoff⁴², P. Renkel⁷⁹, S. Reucroft⁶³, P. Rich⁴⁴, M. Rijssenbeek⁷², I. Ripp-Baudot¹⁸, F. Rizatdinova⁷⁶, S. Robinson⁴³, R.F. Rodrigues³, C. Royon¹⁷, P. Rubinov⁵⁰, R. Ruchti⁵⁵, G. Safronov³⁶, G. Sajot¹³, A. Sánchez-Hernández³², M.P. Sanders¹⁶, A. Santoro³, G. Savage⁵⁰, L. Sawyer⁶⁰, T. Scanlon⁴³, D. Schaile²⁴, R.D. Schamberger⁷², Y. Scheglov³⁹, H. Schellman⁵³, P. Schieferdecker²⁴, T. Schliephake²⁵, C. Schwanenberger⁴⁴, A. Schwartzman⁶⁸, R. Schwienhorst⁶⁵, J. Sekaric⁴⁹, S. Sengupta⁴⁹, H. Severini⁷⁵, E. Shabalina⁵¹, M. Shamim⁵⁹, V. Shary¹⁷, A.A. Shchukin³⁸, R.K. Shivpuri²⁷, D. Shpakov⁵⁰, V. Siccaldi¹⁸, V. Simak⁹, V. Sirotenko⁵⁰, P. Skubic⁷⁵, P. Slattery⁷¹, D. Smirnov⁵⁵, J. Snow⁷⁴, G.R. Snow⁶⁷, S. Snyder⁷³, S. Söldner-Rembold⁴⁴, L. Sonnenschein¹⁶, A. Sopczak⁴², M. Sosebee⁷⁸, K. Soustruznik⁸, M. Souza², B. Spurlock⁷⁸, J. Stark¹³, J. Steele⁶⁰, V. Stolin³⁶, A. Stone⁵¹, D.A. Stoyanova³⁸, J. Strandberg⁶⁴, S. Strandberg⁴⁰, M.A. Strang⁶⁹, M. Strauss⁷⁵, E. Strauss⁷², R. Ströhmer²⁴, D. Strom⁵³, L. Stutte⁵⁰, S. Sumowidagdo⁴⁹, P. Svoisky⁵⁵, A. Sznajder³, M. Talby¹⁴, P. Tamburello⁴⁵, A. Tanasijczuk¹, W. Taylor⁵, P. Telford⁴⁴, J. Temple⁴⁵, B. Tiller²⁴, F. Tissandier¹², M. Titov¹⁷, V.V. Tokmenin³⁵, T. Toole⁶¹, I. Torchiani²², T. Trefzger²³, D. Tsybychev⁷², B. Tuchming¹⁷, C. Tully⁶⁸, P.M. Tuts⁷⁰, R. Unalan⁶⁵, S. Uvarov³⁹, L. Uvarov³⁹, S. Uzunyan⁵², B. Vachon⁵, P.J. van den Berg³³, B. van Eijk³³, R. Van Kooten⁵⁴, W.M. van Leeuwen³³, N. Varelas⁵¹, E.W. Varnes⁴⁵, I.A. Vasilyev³⁸, M. Vaupel²⁵, P. Verdier¹⁹, L.S. Vertogradov³⁵, M. Verzocchi⁵⁰, F. Villeneuve-Seguiet⁴³, P. Vint⁴³, P. Vokac⁹, E. Von Toerne⁵⁹, M. Voutilainen^{67,f}, M. Vreeswijk³³, R. Wagner⁶⁸, H.D. Wahl⁴⁹, L. Wang⁶¹, M.H.L.S Wang⁵⁰, J. Warchol⁵⁵, G. Watts⁸², M. Wayne⁵⁵, M. Weber⁵⁰, G. Weber²³, A. Wenger^{22,g}, N. Wermes²¹, M. Wetstein⁶¹, A. White⁷⁸, D. Wicke²⁵, G.W. Wilson⁵⁸, S.J. Wimpenny⁴⁸, M. Wobisch⁶⁰, D.R. Wood⁶³, T.R. Wyatt⁴⁴, Y. Xie⁷⁷, S. Yacoub⁵³, R. Yamada⁵⁰, M. Yan⁶¹, T. Yasuda⁵⁰, Y.A. Yatsunenko³⁵, K. Yip⁷³, H.D. Yoo⁷⁷, S.W. Youn⁵³, J. Yu⁷⁸, A. Zatserklyaniy⁵², C. Zeitnitz²⁵, D. Zhang⁵⁰, T. Zhao⁸², B. Zhou⁶⁴, J. Zhu⁷², M. Zielinski⁷¹, D. Zieminska⁵⁴, A. Zieminski⁵⁴, L. Zivkovic⁷⁰, V. Zutshi⁵², and E.G. Zverev³⁷

(The $D\bar{0}$ Collaboration)

¹Universidad de Buenos Aires, Buenos Aires, Argentina

²LAFEX, Centro Brasileiro de Pesquisas Físicas, Rio de Janeiro, Brazil

³Universidade do Estado do Rio de Janeiro, Rio de Janeiro, Brazil

⁴Instituto de Física Teórica, Universidade Estadual Paulista, São Paulo, Brazil

⁵University of Alberta, Edmonton, Alberta, Canada,

Simon Fraser University, Burnaby, British Columbia,

Canada, York University, Toronto, Ontario, Canada,

and McGill University, Montreal, Quebec, Canada

⁶University of Science and Technology of China, Hefei, People's Republic of China

⁷Universidad de los Andes, Bogotá, Colombia

⁸Center for Particle Physics, Charles University, Prague, Czech Republic

⁹Czech Technical University, Prague, Czech Republic

¹⁰Center for Particle Physics, Institute of Physics,

Academy of Sciences of the Czech Republic, Prague, Czech Republic

¹¹Universidad San Francisco de Quito, Quito, Ecuador

¹²Laboratoire de Physique Corpusculaire, IN2P3-CNRS,

Université Blaise Pascal, Clermont-Ferrand, France

¹³Laboratoire de Physique Subatomique et de Cosmologie,

IN2P3-CNRS, Université de Grenoble 1, Grenoble, France

¹⁴CPPM, IN2P3-CNRS, Université de la Méditerranée, Marseille, France

¹⁵Laboratoire de l'Accélérateur Linéaire, IN2P3-CNRS et Université Paris-Sud, Orsay, France

¹⁶LPNHE, IN2P3-CNRS, Universités Paris VI and VII, Paris, France

¹⁷DAPNIA/Service de Physique des Particules, CEA, Saclay, France

¹⁸IPHC, Université Louis Pasteur et Université de Haute Alsace, CNRS, IN2P3, Strasbourg, France

¹⁹IPNL, Université Lyon 1, CNRS/IN2P3, Villeurbanne, France and Université de Lyon, Lyon, France

²⁰III. Physikalisches Institut A, RWTH Aachen, Aachen, Germany

²¹Physikalisches Institut, Universität Bonn, Bonn, Germany

²²Physikalisches Institut, Universität Freiburg, Freiburg, Germany

- ²³*Institut für Physik, Universität Mainz, Mainz, Germany*
²⁴*Ludwig-Maximilians-Universität München, München, Germany*
²⁵*Fachbereich Physik, University of Wuppertal, Wuppertal, Germany*
²⁶*Panjab University, Chandigarh, India*
²⁷*Delhi University, Delhi, India*
²⁸*Tata Institute of Fundamental Research, Mumbai, India*
²⁹*University College Dublin, Dublin, Ireland*
³⁰*Korea Detector Laboratory, Korea University, Seoul, Korea*
³¹*SungKyunKwan University, Suwon, Korea*
³²*CINVESTAV, Mexico City, Mexico*
³³*FOM-Institute NIKHEF and University of Amsterdam/NIKHEF, Amsterdam, The Netherlands*
³⁴*Radboud University Nijmegen/NIKHEF, Nijmegen, The Netherlands*
³⁵*Joint Institute for Nuclear Research, Dubna, Russia*
³⁶*Institute for Theoretical and Experimental Physics, Moscow, Russia*
³⁷*Moscow State University, Moscow, Russia*
³⁸*Institute for High Energy Physics, Protvino, Russia*
³⁹*Petersburg Nuclear Physics Institute, St. Petersburg, Russia*
⁴⁰*Lund University, Lund, Sweden, Royal Institute of Technology and Stockholm University, Stockholm, Sweden, and Uppsala University, Uppsala, Sweden*
⁴¹*Physik Institut der Universität Zürich, Zürich, Switzerland*
⁴²*Lancaster University, Lancaster, United Kingdom*
⁴³*Imperial College, London, United Kingdom*
⁴⁴*University of Manchester, Manchester, United Kingdom*
⁴⁵*University of Arizona, Tucson, Arizona 85721, USA*
⁴⁶*Lawrence Berkeley National Laboratory and University of California, Berkeley, California 94720, USA*
⁴⁷*California State University, Fresno, California 93740, USA*
⁴⁸*University of California, Riverside, California 92521, USA*
⁴⁹*Florida State University, Tallahassee, Florida 32306, USA*
⁵⁰*Fermi National Accelerator Laboratory, Batavia, Illinois 60510, USA*
⁵¹*University of Illinois at Chicago, Chicago, Illinois 60607, USA*
⁵²*Northern Illinois University, DeKalb, Illinois 60115, USA*
⁵³*Northwestern University, Evanston, Illinois 60208, USA*
⁵⁴*Indiana University, Bloomington, Indiana 47405, USA*
⁵⁵*University of Notre Dame, Notre Dame, Indiana 46556, USA*
⁵⁶*Purdue University Calumet, Hammond, Indiana 46323, USA*
⁵⁷*Iowa State University, Ames, Iowa 50011, USA*
⁵⁸*University of Kansas, Lawrence, Kansas 66045, USA*
⁵⁹*Kansas State University, Manhattan, Kansas 66506, USA*
⁶⁰*Louisiana Tech University, Ruston, Louisiana 71272, USA*
⁶¹*University of Maryland, College Park, Maryland 20742, USA*
⁶²*Boston University, Boston, Massachusetts 02215, USA*
⁶³*Northeastern University, Boston, Massachusetts 02115, USA*
⁶⁴*University of Michigan, Ann Arbor, Michigan 48109, USA*
⁶⁵*Michigan State University, East Lansing, Michigan 48824, USA*
⁶⁶*University of Mississippi, University, Mississippi 38677, USA*
⁶⁷*University of Nebraska, Lincoln, Nebraska 68588, USA*
⁶⁸*Princeton University, Princeton, New Jersey 08544, USA*
⁶⁹*State University of New York, Buffalo, New York 14260, USA*
⁷⁰*Columbia University, New York, New York 10027, USA*
⁷¹*University of Rochester, Rochester, New York 14627, USA*
⁷²*State University of New York, Stony Brook, New York 11794, USA*
⁷³*Brookhaven National Laboratory, Upton, New York 11973, USA*
⁷⁴*Langston University, Langston, Oklahoma 73050, USA*
⁷⁵*University of Oklahoma, Norman, Oklahoma 73019, USA*
⁷⁶*Oklahoma State University, Stillwater, Oklahoma 74078, USA*
⁷⁷*Brown University, Providence, Rhode Island 02912, USA*
⁷⁸*University of Texas, Arlington, Texas 76019, USA*
⁷⁹*Southern Methodist University, Dallas, Texas 75275, USA*
⁸⁰*Rice University, Houston, Texas 77005, USA*
⁸¹*University of Virginia, Charlottesville, Virginia 22901, USA and*
⁸²*University of Washington, Seattle, Washington 98195, USA*

(Dated: August 15, 2007)

We study the flavor-changing-neutral-current process $c \rightarrow u\mu^+\mu^-$ using 1.3 fb^{-1} of $p\bar{p}$ collisions

at $\sqrt{s} = 1.96$ TeV recorded by the D0 detector operating at the Fermilab Tevatron Collider. We see clear indications of the D_s^+ and $D^+ \rightarrow \phi\pi^+ \rightarrow \mu^+\mu^-\pi^+$ final states with significance greater than four standard deviations above background for the D^+ state. We search for the continuum decay of $D^+ \rightarrow \pi^+\mu^+\mu^-$ in the dimuon invariant mass spectrum away from the ϕ resonance. We see no evidence of signal above background and set a limit of $\mathcal{B}(D^+ \rightarrow \pi^+\mu^+\mu^-) < 3.9 \times 10^{-6}$ at the 90% C.L. This limit places the most stringent constraint on new phenomena in the $c \rightarrow u\mu^+\mu^-$ transition.

PACS numbers: 13.20.Fc, 11.30.Fs, 11.30.Hv, 12.15.Mm

Many extensions of the standard model (SM) provide a mechanism for flavor-changing-neutral-current (FCNC) decays of beauty, charmed, and strange hadrons that could significantly alter the decay rate with respect to SM expectations. Since FCNC processes are forbidden at tree level in the SM, new physics effects could become visible in FCNC processes if the new amplitudes are larger than the higher-order penguin and box diagrams that mediate FCNC decays in the SM. In B meson decays, the experimental sensitivity has reached the SM expected rates for many FCNC processes. In contrast, GIM suppression [1] in D meson decays is significantly stronger and the SM branching fractions are expected to be as low as 10^{-9} [2, 3]. This leaves a large window of opportunity still available to search for new physics in charm decays. There are several models of new phenomena such as SUSY R -parity violation in a single coupling scheme [4] that lead to a tree level interaction mediated by new particles, or little Higgs models with a new up-like vector quark [5] that lead to direct $Z \rightarrow cu$ couplings. In both scenarios deviations from the SM might only be seen in the up-type quark sector, motivating the extension of experimental studies of FCNC processes to the charm sector.

In this Letter we report on a study of FCNC charm decays including the first observation of the decay $D_s^+ \rightarrow \phi\pi^+ \rightarrow \mu^+\mu^-\pi^+$ and the first evidence for the decay $D^+ \rightarrow \phi\pi^+ \rightarrow \mu^+\mu^-\pi^+$ by requiring a dimuon mass window around the nominal ϕ mass. The inclusion of charge conjugate modes is implied throughout the text. At the reported level of statistics, we expect no contributions from two body $D_{(s)}^+$ decays due to the smaller $D_{(s)}^+ \rightarrow \eta$, ρ , and ω branching fractions and the smaller η , ρ , and $\omega \rightarrow \mu^+\mu^-$ branching fractions [6]. The search for the $c \rightarrow u\mu^+\mu^-$ transition in the decay $D^+ \rightarrow \pi^+\mu^+\mu^-$ is performed in the continuum region of the dimuon invariant mass spectrum below and above the ϕ resonance. We focus on the D^+ continuum decay as opposed to similar D_s^+ or Λ_c decays due to the longer lifetime and higher production fraction of the D^+ meson. The study uses a data sample of $p\bar{p}$ collisions at $\sqrt{s} = 1.96$ TeV corresponding to an integrated luminosity of approximately 1.3 fb^{-1} recorded by the D0 detector operating at the Fermilab Tevatron Collider. Similar studies have recently been published by the FOCUS [7] and CLEO-c [8] collaborations, and preliminary results have been presented

by the BaBar [9] collaboration.

D0 is a general purpose detector described in detail in Ref. [10, 11]. Charged particles are reconstructed using a silicon vertex tracker and a scintillating fiber tracker located inside a superconducting solenoidal coil that provides a magnetic field of approximately 2 T. Photons and electrons are reconstructed using the inner region of a liquid argon calorimeter optimized for electromagnetic shower detection. Jet reconstruction and electron identification are further augmented with the outer region of the calorimeter optimized for hadronic shower detection. Muons are reconstructed using a spectrometer consisting of magnetized iron toroids and three super-layers of proportional tubes and plastic trigger scintillators located outside the calorimeter.

The analysis is based on data collected with dimuon triggers. The D0 trigger is based on a three-tier system. The level 1 and 2 dimuon triggers rely on hits in the muon spectrometer and fast reconstruction of muon tracks. The level 3 trigger performs fast reconstruction of the entire event allowing for further muon identification algorithms, matching of muon candidates to tracks reconstructed in the central tracking system, and requirements on the z position of the $p\bar{p}$ interaction.

The selection requirements are determined using PYTHIA [12] Monte Carlo (MC) events to model both $c\bar{c}$ and $b\bar{b}$ production and fragmentation. The EVTGEN [13] MC is used to decay prompt D mesons and secondary D mesons from B meson decay into the $\phi\pi^+$ and $\mu^+\mu^-\pi^+$ intermediate and final states. The detector response is modeled using a GEANT [14] based MC. The dimuon trigger is modeled using a detailed simulation program incorporating all aspects of the trigger logic. Backgrounds are modeled using data in the mass sideband regions around the D meson mass of $1.4 < m(\pi^+\mu^+\mu^-) < 1.6 \text{ GeV}/c^2$ and $2.2 < m(\pi^+\mu^+\mu^-) < 2.4 \text{ GeV}/c^2$.

Muon candidates are required to have segments reconstructed in at least two out of the three muon system super-layers and to be associated with a track reconstructed with hits in both the silicon and fiber trackers. We require that the muon transverse momentum p_T be greater than $2 \text{ GeV}/c$ and the total momentum p to be above $3 \text{ GeV}/c$. The dimuon system is formed by combining two oppositely charged muon candidates that are associated with the same track jet [15], form a well reconstructed vertex, and have an invariant mass $m(\mu^+\mu^-)$

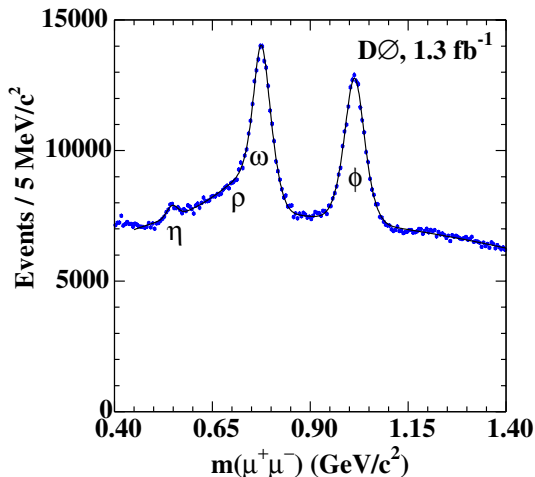


FIG. 1: The inclusive $m(\mu^+\mu^-)$ invariant mass spectrum. The fitting function includes components from the η , ρ , ω , and ϕ resonances.

below $2 \text{ GeV}/c^2$. The dimuon mass distribution in the region of the light quark-antiquark resonances is shown in Fig. 1. Maxima corresponding to the production of ω and ϕ mesons are seen. The ρ is observed as a broad structure beneath the ω peak, and there is some indication of η production as well. For the initial search for resonance dimuon production we require the $\mu^+\mu^-$ mass be within $\pm 0.04 \text{ GeV}/c^2$ of the nominal ϕ mass and re-determine the muon momenta with a ϕ mass constraint imposed [6] which improves the $\mu^+\mu^-\pi^+$ invariant mass resolution by 33%.

Candidate $D_{(s)}^+$ mesons are formed by combining the dimuon system with a track that is associated with the same track jet as the dimuon system, has hits in both the silicon and fiber trackers, and has $p_T > 0.18 \text{ GeV}/c$. The pion impact parameter significance \mathcal{S}_π , defined as the point of closest approach of the track helix to the interaction point in the transverse plane relative to its error, is required to be greater than 0.5. The invariant mass of the three body system must be in the range $1.4 \text{ GeV}/c^2 < m(\pi^+\mu^+\mu^-) < 2.4 \text{ GeV}/c^2$. The three particles must form a well-reconstructed D meson candidate vertex displaced from the primary vertex. The transverse flight length significance \mathcal{S}_D , defined as the transverse distance of the reconstructed D vertex from the primary vertex normalized to the error in the reconstructed flight length, is required to be greater than 5. The collinearity angle Θ_D , defined as the angle between the D momentum vector and the position vector pointing from the primary to the secondary vertex, is required to be less than 500 mrad. In events with multiple $p\bar{p}$ collisions, the longitudinal track impact parameters are used to reject muons and tracks produced in the secondary $p\bar{p}$ interactions. In events with multiple D candidates, the best candidate is chosen based on the χ_{vtx}^2 of the three track vertex and

the angular separation between the pion and the dimuon system in η - ϕ space, $(\Delta R_\pi)^2 = (\Delta\eta)^2 + (\Delta\phi)^2$, which is typically small for true candidates.

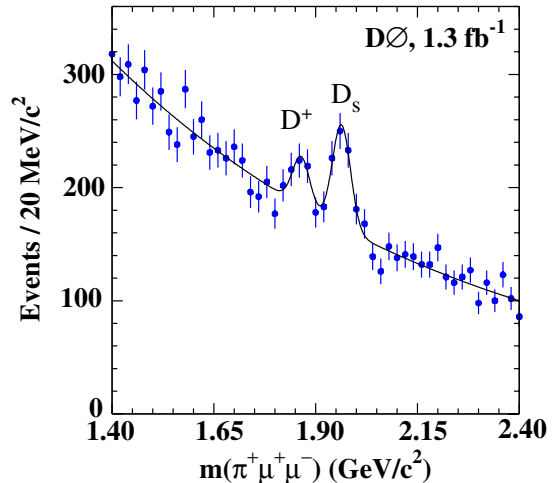


FIG. 2: The $m(\pi^+\mu^+\mu^-)$ mass spectrum in the $0.98 < m(\mu^+\mu^-) < 1.06 \text{ GeV}/c^2$ ϕ mass window. The result of a binned likelihood fit to the distribution including contributions for D^+ , D_s^+ , and combinatoric background is overlaid on the histogram.

The resulting $\pi^+\mu^+\mu^-$ invariant mass distribution is shown in Fig. 2. The $D_{(s)}^+ \rightarrow \phi\pi^+ \rightarrow \mu^+\mu^-\pi^+$ signal is extracted from a binned likelihood fit to the data assuming possible contributions from D^+ and D_s^+ initial states as signal and from combinatoric background. The D_s^+ component is modeled by a Gaussian function with the mean and standard deviation as free parameters. The D^+ component is modeled as a Gaussian function. The difference in means between the D^+ and D_s^+ Gaussian functions is constrained by the known mass difference and the ratio of the standard deviations is constrained to the ratio of masses [6]. The background is modeled as an exponential function with floating parameters. The normalization of all functions are free parameters. The fit yields $254 \pm 36 D_s^+$ candidates and $115 \pm 31 D^+$ candidates. The statistical significance of the combined D_s^+ and D^+ signal is 8 standard deviations above background. The significance of the D^+ yield, treating both the combinatorial and D_s^+ candidates as background, is 4.1 standard deviations.

The relative efficiency of the D^+ and D_s^+ channels is determined separately for prompt D mesons produced in direct $p\bar{p} \rightarrow c\bar{c} + X$ processes and D mesons from B meson decay and combined using the measured prompt fractions [16] $\epsilon^+ = f_p^+ \epsilon_{\text{prompt}}^+ + (1 - f_p^+) \epsilon_{B \rightarrow D}^+$, where $\epsilon_{\text{prompt}}^+$ is the efficiency for prompt D^+ mesons, $\epsilon_{B \rightarrow D}^+$ is the efficiency for D^+ mesons from B meson decay, and f_p^+ is the fraction of prompt D^+ mesons; we use equivalent expressions for D_s^+ mesons. The yield ratio is related to

TABLE I: External inputs to the yield ratio calculation. All numbers have been corrected for the most recent $D^+ \rightarrow K^+\pi^+\pi^-$ and $D_s^+ \rightarrow \phi\pi^+$ branching fractions [6].

f_p^+ [16]	0.891 ± 0.004
f_p^s [16]	0.773 ± 0.038
$f_{c \rightarrow D}^s / f_{c \rightarrow D}^+$ [17]	0.40 ± 0.09

the ratio of branching fractions by

$$\frac{n(D^+)}{n(D_s^+)} = \frac{f_{c \rightarrow D}^+ f_p^+ \epsilon^+ \mathcal{B}(D^+ \rightarrow \phi\pi^+ \rightarrow \mu^+\mu^-\pi^+)}{f_{c \rightarrow D}^s f_p^s \epsilon^s \mathcal{B}(D_s^+ \rightarrow \phi\pi^+) \mathcal{B}(\phi \rightarrow \mu^+\mu^-)},$$

where $f_{c \rightarrow D}^+$ is the fraction of D^+ mesons produced in c quark fragmentation, and $f_{c \rightarrow D}^s$ is the equivalent fraction for D_s^+ mesons [17]. The relevant numbers are listed in Table I. The efficiency ratio is determined from MC to be $\epsilon^s/\epsilon^+ = 0.70 \pm 0.06$ (stat + sys). The difference from unity is caused by the lifetime difference between D_s^+ ($c\tau = 147.0 \mu\text{m}$) and D^+ ($c\tau = 311.8 \mu\text{m}$) mesons, and the systematic uncertainty is dominated by uncertainties in the resolution modeling of \mathcal{S}_D and \mathcal{S}_π .

Using the efficiency ratio, production fractions, and the $D_s^+ \rightarrow \phi\pi^+$ and $\phi \rightarrow \mu^+\mu^-$ branching fractions gives $\mathcal{B}(D^+ \rightarrow \phi\pi^+ \rightarrow \mu^+\mu^-\pi^+) = (1.8 \pm 0.5 \text{ (stat.)} \pm 0.6 \text{ (sys.)}) \times 10^{-6}$, which is consistent with the expected value of $(1.86 \pm 0.26) \times 10^{-6}$ given by the product of the $D^+ \rightarrow \phi\pi^+$ and $\phi \rightarrow \mu^+\mu^-$ branching fractions and other recent measurements [8, 9]. The systematic uncertainty is overwhelmingly dominated by the uncertainty in the $D_s^+ \rightarrow \phi\pi^+$ branching fraction that enters both the normalization and $f_{c \rightarrow D}^s$.

We now turn to the search for the continuum decay of $D^+ \rightarrow \pi^+\mu^+\mu^-$ mediated by FCNC interactions. We study the dimuon invariant mass region below 1.8 GeV/c^2 , excluding $0.96 < m(\mu^+\mu^-) < 1.06 \text{ GeV}/c^2$. Backgrounds are further reduced by requirements on the \mathcal{S}_D , \mathcal{S}_π , Θ_D , χ_{vtx}^2 , and ΔR_π variables defined above. The pion transverse momentum $p_T(\pi)$ and the isolation defined as $\mathcal{I}_D = p(D)/\sum p_{\text{cone}}$ where the sum is over tracks in a cone centered on the D meson of radius $\Delta R = 1$ are also used. The final requirements are chosen using a random grid search [18] optimized using the Punzi [19] criteria to give the optimal 90% C.L. upper limit. The final requirements along with the number of candidates surviving each requirement are listed in Table II.

The $\pi^+\mu^+\mu^-$ invariant mass distribution in data for the dimuon invariant mass region below 1.8 GeV/c^2 excluding $0.96 < m(\mu^+\mu^-) < 1.06 \text{ GeV}/c^2$ is shown in Fig. 3. The D^+ signal region contains 19 events. The combinatorial background in the signal region is estimated by performing sideband extrapolations to be 25.8 ± 4.6 events. The uncertainty reflects the range in the background estimation from variation in the background shape across the $\pi^+\mu^+\mu^-$ mass spectrum. The

TABLE II: Final requirements for the background suppression variables along with the number of candidates surviving each requirement for the continuum $D^+ \rightarrow \pi^+\mu^+\mu^-$ analysis.

	Requirement	Surviving candidates
Preselection		
ΔR_π	< 2.6	154131
$p_T(\pi)$	$> 0.4 \text{ GeV}/c$	127027
\mathcal{S}_D	> 9.4	69817
\mathcal{S}_π	> 1.8	51736
\mathcal{I}_D	> 0.7	24742
Θ_D	$< 7 \text{ mrad}$	962
χ_{vtx}^2 (3 DOF)	< 2.6	212
Signal window	$\pm 2\sigma$	19

probability of the background fluctuating to the measured event yield or fewer events is 14%.

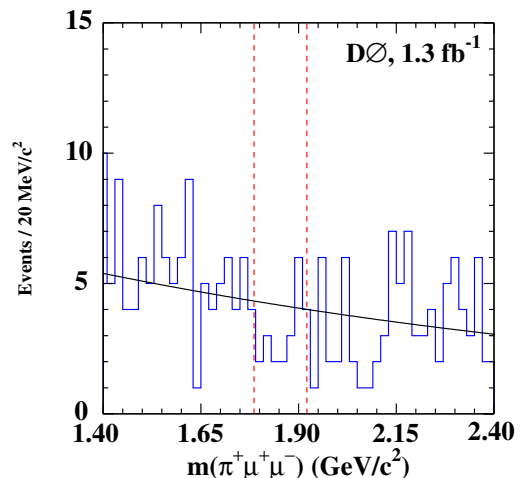


FIG. 3: Final $\pi^+\mu^+\mu^-$ invariant mass spectrum. The $\pm 2\sigma$ D^+ signal region, within the dashed lines, contains 19 events. The background level determined from the sidebands is 25.8 ± 4.6 events.

We normalize the results to the $D^+ \rightarrow \phi\pi^+ \rightarrow \mu^+\mu^-\pi^+$ signal instead of the larger D_s^+ signal to avoid the uncertainties associated with the D^+ and D_s^+ production fractions. We use the product of the known $D^+ \rightarrow \phi\pi^+$ and $\phi \rightarrow \mu^+\mu^-$ branching fractions [6]. The signal efficiency ratio between the $D^+ \rightarrow \pi^+\mu^+\mu^-$ channel in the final sample and the $D^+ \rightarrow \phi\pi^+ \rightarrow \mu^+\mu^-\pi^+$ channel in the preselection sample is determined from MC to be $(5.4 \pm 0.8)\%$. The inputs to the limit calculation are summarized in Table III. The systematic uncertainty is dominated by the modeling of the vertex resolution particularly in the χ_{vtx}^2 requirement. Using this, we find

$$\frac{\mathcal{B}(D^+ \rightarrow \pi^+\mu^+\mu^-)}{\mathcal{B}(D^+ \rightarrow \phi\pi^+) \times \mathcal{B}(\phi \rightarrow \mu^+\mu^-)} < 2.09, \quad 90\% \text{ C.L.}$$

The limit is determined using a Bayesian technique [20]. Using the central value of $D^+ \rightarrow \phi\pi^+$ and $\phi \rightarrow \mu^+\mu^-$

TABLE III: Inputs to the $\mathcal{B}(D^+ \rightarrow \pi^+\mu^+\mu^-)$ upper limit calculation and resulting upper limit at the 90% and 95% C.L.

$D^+ \rightarrow \pi^+\mu^+\mu^-$ candidate yield	19 events
Background expectation	25.8 ± 4.6 events
$D^+ \rightarrow \phi\pi^+ \rightarrow \pi^+\mu^+\mu^-$ candidate yield	115 ± 31 events
Relative efficiency	0.054 ± 0.008
$\mathcal{B}(D^+ \rightarrow \phi\pi^+)$	6.50×10^{-3}
$\mathcal{B}(\phi \rightarrow \mu^+\mu^-)$	2.86×10^{-4}
Single event sensitivity	3.0×10^{-7}
$\mathcal{B}(D^+ \rightarrow \pi^+\mu^+\mu^-)$ 95% C.L.	$< 6.1 \times 10^{-6}$
$\mathcal{B}(D^+ \rightarrow \pi^+\mu^+\mu^-)$ 90% C.L.	$< 3.9 \times 10^{-6}$

branching fractions gives

$$\mathcal{B}(D^+ \rightarrow \pi^+\mu^+\mu^-) < 3.9 \times 10^{-6}, \quad 90\% \text{ C.L.}$$

This is approximately 30% below the limit one would expect to set given an expected background of 25.8 ± 4.6 events. The single event sensitivity, given by the branching fraction one would derive based on one observed signal candidate, is 3.0×10^{-7} .

In conclusion, we have performed a detailed study of D^+ and D_s^+ decays to the $\pi^+\mu^+\mu^-$ final state. We clearly observe the $D_s^+ \rightarrow \phi\pi^+$ intermediate state and see evidence for the $D^+ \rightarrow \phi\pi^+$ intermediate state. The branching fraction for the $D^+ \rightarrow \phi\pi^+ \rightarrow \pi^+\mu^+\mu^-$ final state is consistent with the product of $D^+ \rightarrow \phi\pi^+$ and $\phi \rightarrow \mu^+\mu^-$ branching fractions. We have performed a search for the continuum decay of $D^+ \rightarrow \pi^+\mu^+\mu^-$ by excluding the region of the dimuon invariant mass spectrum around the ϕ . We see no evidence of signal above background and set a limit of $\mathcal{B}(D^+ \rightarrow \pi^+\mu^+\mu^-) < 3.9 \times 10^{-6}$ at the 90% C.L. This is the most stringent limit to date in a decay mediated by a $c \rightarrow u\mu^+\mu^-$ transition. Although this is approximately 500 times above the SM expected rate, it already reduces the allowed parameter space of the product of SUSY R -parity violating couplings $\lambda'_{22k} \times \lambda'_{21k}$ [2]. However, it is still an order of magnitude above the expected level from little Higgs models [5].

We thank the staffs at Fermilab and collaborating institutions. We also thank Sandip Pakvasa for several useful discussions. We acknowledge support from the DOE and NSF (USA); CEA and CNRS/IN2P3 (France); FASI, Rosatom and RFBR (Russia); CAPES, CNPq, FAPERJ, FAPESP and FUNDUNESP (Brazil); DAE and DST (India); Colciencias (Colombia); CONACyT (Mexico); KRF and KOSEF (Korea); CONICET and UBACyT (Argentina); FOM (The Netherlands); Science and Technology Facilities Council (United Kingdom); MSMT and GACR (Czech Republic); CRC Program, CFI, NSERC and WestGrid Project (Canada); BMBF and DFG (Germany); SFI (Ireland); The Swedish Research Council (Sweden); CAS and CNSF (China); Alexander von Humboldt Foundation; and the Marie Curie Program.

- [a] Visitor from Augustana College, Sioux Falls, SD, USA.
- [b] Visitor from The University of Liverpool, Liverpool, UK.
- [d] Visitor from ICN-UNAM, Mexico City, Mexico.
- [e] Visitor from II. Physikalisches Institut, Georg-August-University Göttingen, Germany
- [f] Visitor from Helsinki Institute of Physics, Helsinki, Finland.
- [g] Visitor from Universität Zürich, Zürich, Switzerland. Universität Zürich, Zürich, Switzerland.
- [†] Fermilab International Fellow
- [‡] deceased

- [1] S. L. Glashow, J. Iliopoulos, and L. Maiani Phys. Rev. D **2**, 1285 (1970).
- [2] G. Burdman, E. Golowich, J. Hewett, and S. Pakvasa, Phys. Rev. D **66**, 014009 (2002).
- [3] S. Fajfer, S. Prelovsek, and P. Singer, Phys. Rev. D **64**, 114009 (2001).
- [4] K. Agashe and M. Graesser, Phys. Rev. D **54**, 4445 (1996).
- [5] S. Fajfer and S. Perlovsek, Phys. Rev. D **73**, 054026 (2006).
- [6] W.-M. Yao *et al.* (Particle Data Group), Journal of Physics G **33**, 1 (2006).
- [7] J. M. Link *et al.* (FOCUS Collaboration), Phys. Lett. B **572**, 21 (2003).
- [8] Q. He *et al.* (CLEO Collaboration), Phys. Rev. Lett. **95**, 221802 (2005).
- [9] B. Aubert *et al.* (BaBar Collaboration) BABAR-CONF-06/04, SLAC-PUB-11948, hep-ex/0607051, submitted to the Proceedings of ICHEP2006
- [10] V.M. Abazov *et al.* (DO Collaboration), Nucl. Instrum. Methods A **565**, 463 (2006).
- [11] V.M. Abazov *et al.* (DO Collaboration), Nucl. Instrum. Methods A **552**, 372 (2005).
- [12] T. Sjostrand *et al.*, Computer Phys. Commun. **135**, 238 (2001).
- [13] D. J. Lange, Nucl. Instrum. Methods A **462**, 152 (2001).
- [14] R. Brun, F. Bruyant, M. Maire, A. C. McPherson, and P. Zancarini, CERN DD/EE/84-1 (1987).
- [15] All charged particles in the event are clustered into jets using the DURHAM clustering algorithm with the p_T cut-off parameter of 15 GeV/c. S. Catani *et al.*, Phys. Lett. B **269**, 432 (1991).
- [16] D. Acosta *et al.* (CDF Collaboration), Phys. Rev. Lett. **91**, 241804 (2003).
- [17] S. Chekanov *et al.* (ZEUS Collaboration), Eur. Phys. J. **C44**, 351 (2005). We rescale the values to be consistent with the $D^+ \rightarrow K^+\pi^+\pi^-$ and $D_s^+ \rightarrow \phi\pi^+$ branching fractions in Ref. [6].
- [18] N. Amos *et al.* in *Proc. of Computing in High Energy Physics (CHEP'95)*, edited by R. Shellard and T. Nguyen (World Scientific, River Edge, NJ, 1996), p. 215.
- [19] G. Punzi in *Proc. of the Conference on Statistical Problems in Particle Physics, Astrophysics and Cosmology (Phystat 2003)*, edited by L. Lyons *et al.* (SLAC, Menlo Park, CA, 2003), p. 79.
- [20] I. Bertram *et al.*, FERMILAB-TM-2104 (2000).